SSRG International Journal of Electronics and Communication Engineering
ISSN: 2348-8549/ https://doi.org/10.14445/23488549/IJECE-V12I12P115

Volume 12 Issue 12, 177-188, December 2025

Original Article

Vibration Analysis of Cantilever Beams Using Deep Learning Enhanced Photodiode Non-Uniformity

Honey Devassy[1], L.D. Vijay Anand[2], Hepsiba D[3]

[1,2]*Department of Robotics Engineering, Karunya Institute of Technology and Sciences, Coimbatore, Tamil Nadu, India.*
[3]*Department of Biomedical Engineering, Karunya Institute of Technology and Sciences, Coimbatore, Tamil Nadu, India.*

[1]*Corresponding Author : honeydevassy@karunya.edu.in*

Received: 15 October 2025 Revised: 16 November 2025 Accepted: 15 December 2025 Published: 27 December 2025

Abstract *- Conventional vibration monitoring techniques for cantilever beams suffer from several limitations, including physical contact requirements, installation complexity, degradation over time, and susceptibility to environmental noise. Photodiodes, while commonly used in optical sensing, are typically assumed to exhibit uniform responsivity. Additionally, traditional approaches offer limited scalability for real-time, non-invasive, and predictive maintenance solutions. This paper presents a novel vibration analysis technique that exploits the non-uniform spectral responsivity of photodiodes to detect beam oscillations without physical contact. When a vibrating cantilever beam reflects a laser spot across the photodiode surface, spatial variations in light incidence produce voltage fluctuations that are recorded using a digital storage oscilloscope. Experiments conducted on different cantilever beams reveal that the proposed method accurately determines natural frequencies. To enhance diagnostic accuracy, the voltage signals are processed using a Deep Learning Model, Sentiment Cross-Fusion Network (SCFN), optimized with the Improvised Arctic Fox Algorithm (IAFA). Among competing models, the sentiment cross-fusion network achieved the highest classification accuracy of 0.90%. The improvised arctic fox algorithm further improved prediction performance, achieving 92.1% accuracy, with the lowest error values of root mean square error (0.10) and mean absolute error (0.07). The proposed framework demonstrates excellent potential for real-time, scalable, and accurate structural health monitoring in civil and industrial applications, although considerations like photodiode alignment and active area limitations must be addressed for broader deployment.*

Keywords *- Vibration Analysis, Cantilever Beam, Photodiode Non-Uniformity, Deep Learning, Optimization.*

1. Introduction

Beams form the backbone of many structural and mechanical systems, serving as critical elements in load distribution, stability, and dynamic performance. From bridges, buildings, and cranes to aircraft wings and precision instruments, the role in resisting bending and vibrational forces is indispensable. In particular, cantilever beams, fixed at one end and free at the other, are frequently employed in engineering structures such as balconies, overhangs, robotic arms, and biomedical equipment due to the ability to support extended spans without intermediate support. Monitoring the vibrational behaviour of cantilever beams is vital for ensuring structural integrity, especially under dynamic loading.

Vibration analysis of beams [1-4] enables early detection of defects such as cracks, material fatigue, and stiffness degradation, making it a cornerstone of predictive maintenance strategies in both civil and industrial domains. Classical beam theories, such as the Euler-Bernoulli, Timoshenko, and Rayleigh models, provide valuable insight into beam dynamics under various boundary and material conditions. However, discrepancies often arise between theoretical predictions and experimental observations due to damping, non-linearities [5, 6], and real-world imperfections [7-9]. Traditional vibration sensing techniques often rely on contact-based methods, including piezoelectric sensors and accelerometers [10-12]. While effective, these systems may suffer from drawbacks such as signal distortion due to physical contact, sensitivity to environmental noise, and limitations in measuring out-of-plane motion.

To overcome these challenges, non-contact optical sensing techniques [13] have gained popularity due to high sensitivity, immunity to electromagnetic interference, and capacity for remote monitoring. Most of the optical methods of vibration measurement include a photodiode, which is intended only for light detection. In this research, a novel optical sensing method is presented for vibration analysis of cantilever beams by exploiting the inherent non-uniformity in the spectral responsivity of photodiodes. The advantage of the method is that the Photodiode itself acts as a vibration sensor, thereby reducing the number of optical components required

in existing optical approaches. Unlike conventional photodiode-based systems that assume uniform sensitivity across the active area, this research harnesses the natural spatial non-uniformity in the device response. When a vibrating cantilever beam reflects a laser beam onto the photodiode surface, the changing position of incidence due to beam deflection results in corresponding voltage variations. These voltage signals are recorded in real-time and analysed to extract natural frequencies of the beam under free vibration. The proposed technique is validated through experimental research on cantilever beams of different materials (stainless steel, aluminium, and galvanized iron), with comparisons drawn against analytical calculations, simulation results from ANSYS, and experimentation with an accelerometer. By utilizing a minimalistic and cost-effective setup, this approach offers a scalable and accurate non-contact solution for monitoring structural vibrations, paving the way for improved safety, diagnostics, and reliability in structural health monitoring systems.

2. Literature Review

Vibration-based structural monitoring is a well-established method in the field of engineering. Li et al. [14] and Nguyen et al. [15] elucidated the essential function of vibration analysis in the evaluation of the condition of civil and mechanical structures. The cracks change the characteristics of the beam. Chinka et al. [16] and Pathak, D et al. [17] explicated the vibration behaviour of cracked beams simulated in ANSYS, explaining that crack dimensions substantially influence the natural frequencies. Khatir, A et al. [18] explained a hybrid PSO-YUKI algorithm integrated with radial basis functions for locating double cracks in CFRP beams using experimental and FEM-based vibrational data. The remarkable accuracy and computational efficiency in crack depth detection are demonstrated in this paper. Machine learning based damage detection of beams has gained traction due to its ability to enhance accuracy and efficiency in structural health monitoring. Feng, H et al. [19] and Afandi et al. [20] demonstrated various methodologies leveraging Deep Learning, Data Augmentation, and Hybrid Algorithms to address the challenges of traditional inspection methods.

Siva et al. [21] proposed two methodologies for crack detection: one utilizing digital image processing and the other employing deep learning with Convolutional Neural Networks (CNNs) for detection and ResNet for classification, demonstrating superior accuracy over existing techniques on publicly available datasets. Harikumar, V et al. [22] explained a digital twin framework for beams using support vector machines, incorporating stiffness degradation and damage evolution over dual time scales. Zhang, X et al. [23] introduced a Fourier Transformation-based Physics-Informed Neural Network (FT-PINN) to accurately predict the dynamic responses of cantilever beams under complex excitations. Katam, R et al. [24] combined vibration-based analysis with support vector machines to improve damage detection in cantilever beams, addressing the limitations of frequency-based methods. The approach achieved 85% accuracy in identifying damage across varying locations and severities, demonstrating improved robustness over traditional techniques. The literature survey shows that the integration of artificial intelligence into the traditional approaches will enhance the accuracy of any measurement. In this paper, a novel, deep learning enhanced photodiode non-uniform based optical method is presented for vibration analysis of cantilever beams.

2.1. Problem Statement

Traditional contact-based sensor-based vibration monitoring systems for cantilever beams are limited by complex installation, vulnerability to environmental noise, and degradation over time. These limitations demand non-invasive solutions and lead to the wide use of non-contact optical-based approaches. Photodiodes are an integral part of almost all optical-based vibration monitoring systems. Furthermore, while conventional photodiodes are used in optical sensing applications, the assumed uniform responsivity across the surface fails to exploit the full potential for vibration detection. The lack of intelligent, real-time fault identification further delays maintenance responses. Therefore, there is a critical need for a novel, accurate, non-contact vibration sensing method that leverages photodiode non-uniformity and integrates advanced deep learning models to enable predictive maintenance, early fault detection, and continuous monitoring of cantilever beam structures. This research introduces a novel non-contact vibration monitoring technique that leverages the non-uniform responsivity of photodiodes, transforming an optical irregularity into a sensing advantage. It integrates a Deep Learning Model-SCFN, optimized by the IAFA for real-time structural fault detection. The method is experimentally validated on different cantilever beams and cross-verified with analytical, simulation, and accelerometer data. The materials and methods will be presented in Section 3, the results with analysis in Section 4, and the conclusion in Section 5.

3. Methodology

The spectral responsivity of the Photodiode reveals its inherent non-uniformity, wherein the output voltage varies based on the exact point of light incidence on its active region. While most photodiode applications assume uniform responsivity, especially in light intensity measurements, this research focuses on exploiting the nonlinear, spatially varying response. A novel, non-contact, photodiode-based optical vibration measurement technique is developed for cantilever beams. The natural frequencies of cantilever beams made of various materials, such as stainless steel SS304, Aluminium, and galvanized iron, are determined using this approach. Free vibrations through a small displacement are induced into the beams, and real-time photodiode signals are captured via a

Digital Storage Oscilloscope (DSO). The results are validated analytically, using modal analysis using ANSYS and using an ADXL335 accelerometer interfaced with an Arduino UNO. The consistency across all methods confirms the accuracy and reliability of the proposed technique.

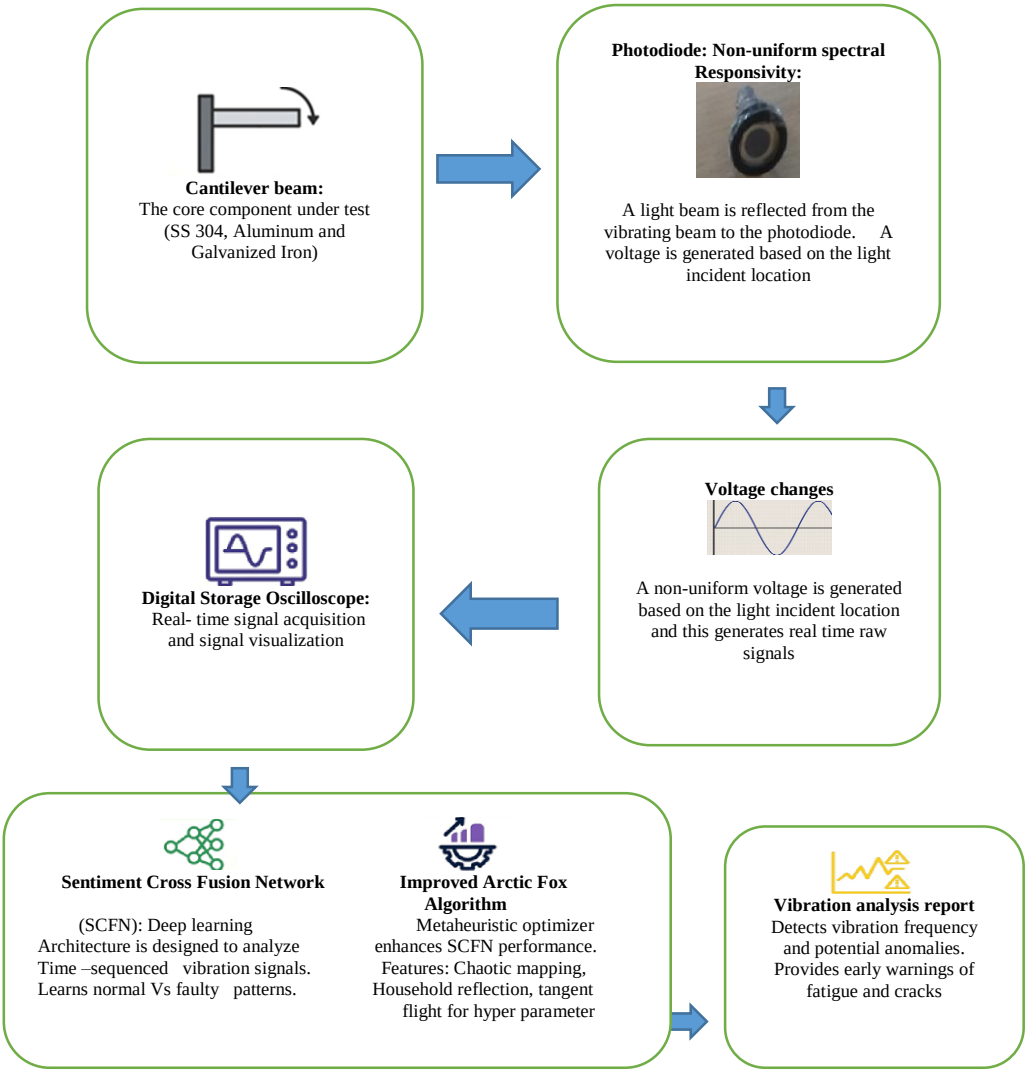

Fig. 1 Proposed methodology for vibration analysis

Figure 1 illustrates the complete flow of the proposed vibration analysis system for cantilever beams using photodiode non-uniformity enhanced by Deep Learning. The process begins with a cantilever beam (made of SS304, Aluminium, or Galvanized iron) that is set into free vibration by a slight displacement. A small mirror is attached to the vibrating beam, and a laser beam is directed towards the mirror. The reflected beam is detected by a photodiode. As the beam vibrates, the incident position of the beam on the surface of the Photodiode varies. The non-uniform characteristics of the Photodiode thus generate a changing voltage that depends on the vibrational frequency of the beam. These voltage fluctuations are observed in real time using a DSO. These raw vibration data are then fed into an SCFN, which analyses the vibrational data to identify the faulty structural behaviour. Applying a metaheuristic optimizer incorporating chaotic mapping, Householder reflection, and tangent flight strategies, the performance of SCFN is further enhanced by the IAFA. The final output of this integrated system makes it a robust tool for predictive maintenance and structural health monitoring.

The specifications as well as the properties of three Cantilever Beams under research are given in Tables 1 and 2.

Table 1. Specifications of cantilever beams

Length of beam, L	900mm
Breadth, b	40mm
Thickness of beam, h	1mm

Table 2. Material properties of beams

Material of the Beam	Modulus of Elasticity, GPa	Density kg/m3
Aluminium	70	2700
Stainless steel	200	8000
Galvanized iron	210	7870

3.1. Photodiode Non-Uniformity Analysis

To explore the non-uniform spectral responsivity of the Photodiode, a laser source of 635 nm is utilized. The setup, as shown in Figure 2, includes the laser module and the Photodiode used for the experiment. The laser is powered with a constant voltage of 7V to ensure stable beam output during the scanning process. The laser beam is directed at the active surface of the Photodiode, and its spatial responsivity is characterized by moving the beam gradually across the detector's surface, specifically through its central region from one end to the other. At each scanned position, the resulting output voltage is measured using a digital multimeter to capture the variations in responsivity due to non-uniform light sensitivity across the surface. This scanning procedure is repeated multiple times to ensure repeatability, and the observed variations in voltage confirm the inherent non-uniformity of the Photodiode. The characteristic output responses obtained from this scanning process are depicted in Figure 3.

Fig. 2 Photodiode and laser used for the experiment

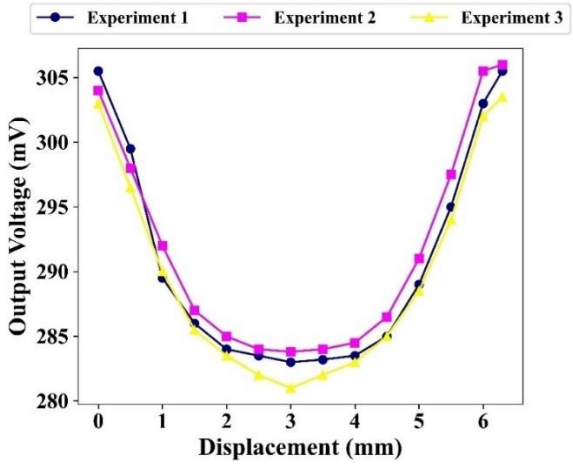

Fig. 3 Spectral responsivity of photodiode

3.2. Determination of Natural Frequency Analytically

The natural frequency of a free-vibrated beam is purely dependent on the system parameters of mass and stiffness. A few assumptions, like lumped mass at the free end, undamped vibrations, etc., have been made when a real-time system is approximated to a simple beam.

A cantilever beam subjected to free vibrations, as described based on Euler-Bernoulli's Beam Theory, is given by Equation (1).

$$\frac{d^2}{dx^2}\left\{ EI\frac{d^2Y(x)}{dx^2}\right\} = \omega_n m(x)Y(x) \quad (1)$$

Where E represents the rigidity modulus of the beam, I represents the moment of inertia, Y(x) represents displacement in the y direction, ω_n represents the circular natural frequency, and m represents the mass per unit length.

Analytically, Euler-Bernoulli Beam Theory is applied to deduce natural frequencies of cantilever beams under various modes. The frequency of a beam for an nth mode is given by Equation (2).

$$\omega_n = \sqrt{\frac{k}{m}} \quad (in\ rad/\text{sec}) \quad (2)$$

Where m represents the modal mass, and k represents the stiffness.

To determine the natural frequencies of three beams analytically, the modal mass and stiffness are needed. These parameters are calculated first from the specifications and material properties of the beam. Equations (3) and (4) are used for this purpose.

$$k = \frac{3EI}{L^3} \quad (3)$$

$$I = \frac{\mathrm{b}h^3}{12} \quad (4)$$

Then, the natural frequency of vibrations of three Cantilever Beams under research is determined analytically using Equation (2).

3.3. Determination of the Natural Frequency of Beam Using ANSYS software

The Cantilever Beams under research are analysed using the modal analysis software, and the natural frequency of the beams is obtained. The three-dimensional finite element models of Cantilever Beams are constructed, and Computational Modal analysis on ANSYS-17 is then performed to generate various mode shapes. The natural frequency is thus observed. Modal analysis of a beam made of SS304 is presented in Figures 4 and 5. Similarly, the Cantilever Beams of Aluminium and Galvanized Iron are modelled, and the natural frequencies are calculated.

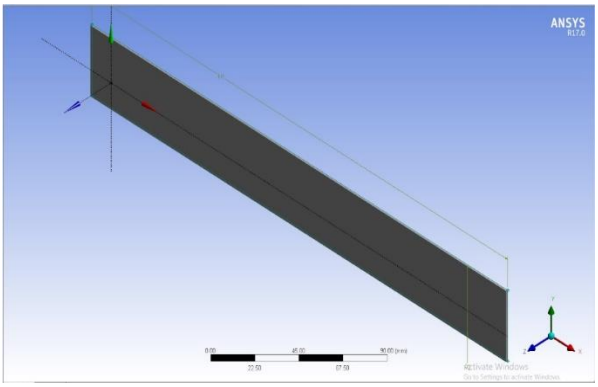

Fig. 4 Model of stainless-steel cantilever beam in ANSYS

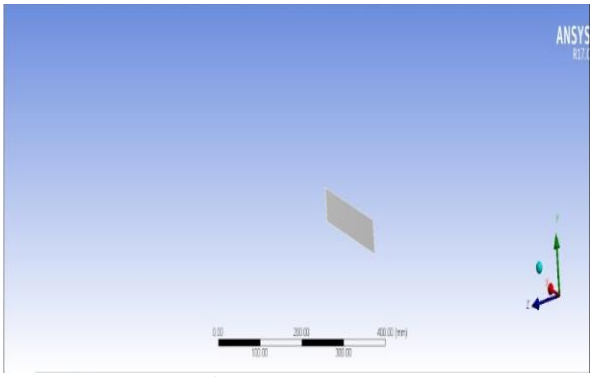

Fig. 5 Modal analysis of stainless-steel cantilever beam in ANSYS

3.4. Cantilever Beam Vibration Measurement Using ADXL335 Accelerometer

The ADXL335 accelerometer is a widely used sensor for vibration measurement due to its compact design, low power consumption, and three-axis sensing capabilities [25]. The ADXL335 outputs voltages proportional to acceleration in the X, Y, and Z axes. It is known for its high sensitivity and low cross-axis sensitivity, making it suitable for precise vibration measurements. The sensor operates on a voltage of 3.3 V or 5 V and has a typical current consumption of 300 μA. The frequency of vibration of the cantilever under research is measured using ADXL335 integrated with Arduino UNO. Since the vibration of the beam is in the Z direction, the z-axis reading of ADXL335 is required. The five pins of ADXL335 are Vcc, GND, X, Y, and Z. ADXL335 is connected to Arduino UNO, and the pin connections are shown in Table 3. As ADXL335 is an analog accelerometer, the Z pin of the device is connected to A0 of the Arduino UNO. The vibrating pattern of the beam is observed in real time using a serial plotter on Arduino. The same vibrations are captured by DSO. Figure 6 shows the experimental setup for the ADXL335 accelerometer.

Table 3. Pin connections of ADXL335 and Arduino

ADXL335 Pin	Arduino Pin
Vcc	3.3V
GND	GND
Z	A0

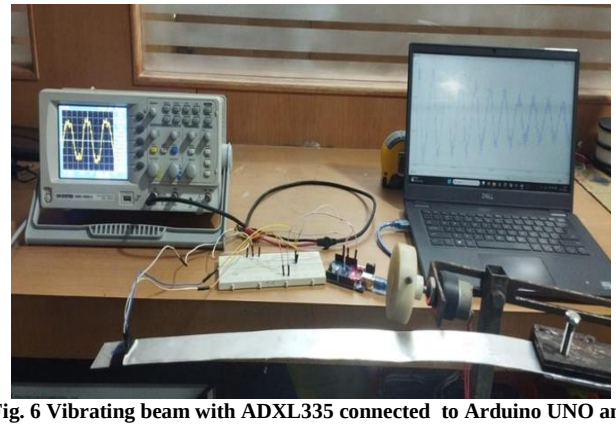

Fig. 6 Vibrating beam with ADXL335 connected to Arduino UNO and DSO

3.4.1. Waveforms Observed during Measurement using ADXL335 Accelerometer

An ADXL335 accelerometer is attached to the Cantilever Beam, and the beam is allowed to vibrate at its natural frequency. When the beam vibrates, the accelerometer experiences the same vibrations in the Z-axis. This periodic movement of the Z-axis is transferred to Arduino UNO via analog pin A0. The same vibrations are observed in the DSO, which is connected to the accelerometer. Thus, the frequency of vibrations is measured and recorded.

The vibrations of the beam are plotted using a serial plotter on Arduino. The experiment is performed for SS, Aluminium, and GI cantilever beams for beam lengths of 300mm, 400mm, and 500mm.

Figure 7 shows the vibrations obtained using ADXL335 along with Arduino for an Aluminium beam for a beam length of 300mm. When the beam is displaced to induce vibrations, the amplitude of vibration is high. Gradually, the amplitude of vibrations decays and reaches a steady state where the beams vibrate with natural frequency.

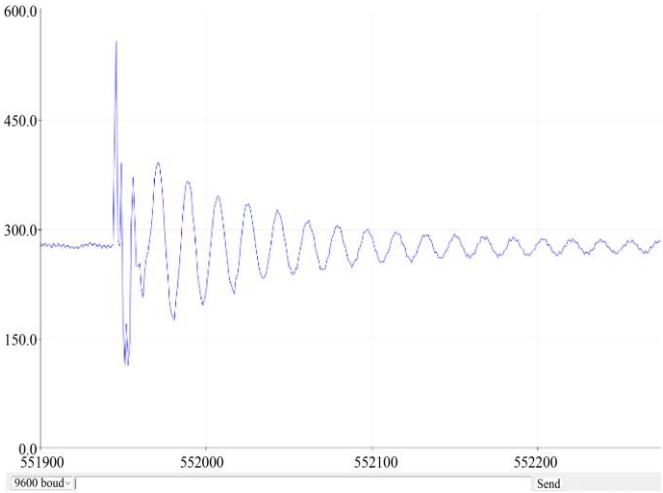

Fig. 7 Aluminium beam vibrations observed in serial plotter for a beam length of 300mm

3.5. Cantilever Beam Vibration Measurement Using Photodiode

In this section, the non-uniformity of the Photodiode is used to monitor the vibration of Cantilever Beams. The experiment is performed with three Cantilever Beams of Aluminium, Stainless steel, and Galvanized Iron. The arrangement of the components of vibration measurement is shown in Figure 8. A small mirror is attached to the cantilever beam. A laser beam from the laser source is allowed to fall on the mirror and is reflected towards the Photodiode. When the Cantilever Beam vibrates, the reflected laser beam from the mirror falls on various positions in the active region of the Photodiode. Due to non-uniformity, different voltages are generated in the Photodiode. i.e., The vibration of the beam modulates the incident position of light on the Photodiode and generates output voltage accordingly. Thus, the non-uniformity of the Photodiode is effectively applied to detect the frequency of vibration of the beam.

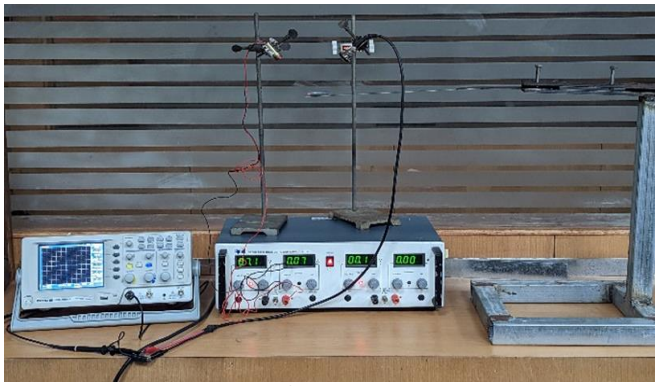

Fig. 8 Experimental setup of the proposed vibration measurement technique

When the beam is given a small displacement, it starts to vibrate. Initially, it vibrates with a higher amplitude, but the inherent damping of the system decays the amplitude of free vibration. The natural frequency of the beam is measured when a stable condition is observed. When the cantilever beam vibrates, it follows a periodic, to-and-fro motion, and so the vibration-modulated laser beam received by the Photodiode follows the same pattern.

As a result, the waveforms observed in the DSO during vibration measurement using a photodiode are sinusoidal signals. Since the natural frequency of free vibration is in the range of very few Hz, there is a chance of distortion as observed in the waveforms. The natural frequency of the beams is noted directly from the DSO. The waveforms obtained from DSO for a stainless steel beam of length 300mm, 400mm, and 500mm.

3.5.1. Waveforms Observed During Measurement using Photodiode

When the beam is given a small displacement, it starts to vibrate. Initially, it vibrates with a higher amplitude, but the inherent damping of the system decays the amplitude of free vibration. The natural frequency of the beam is measured when a stable condition is observed. The vibration-modulated laser beam is received by the Photodiode, which follows the periodic movement of the beam pattern. As a result, the waveforms observed in the DSO during vibration measurement using a photodiode are sinusoidal signals.

Since the natural frequency of free vibration is in the range of very few Hz, there is a chance of distortion as observed in the waveforms. The natural frequency of the beams is noted directly from the DSO. Figure 9 presents the waveforms captured via DSO for a stainless steel cantilever beam of length 300mm. As presented in the Figure, the corresponding natural frequencies are observed to be 8.591 Hz. Similarly, Figures 10 and 11 show the waveforms captured via DSO for Aluminium and GI cantilever beams of beam lengths 500mm.

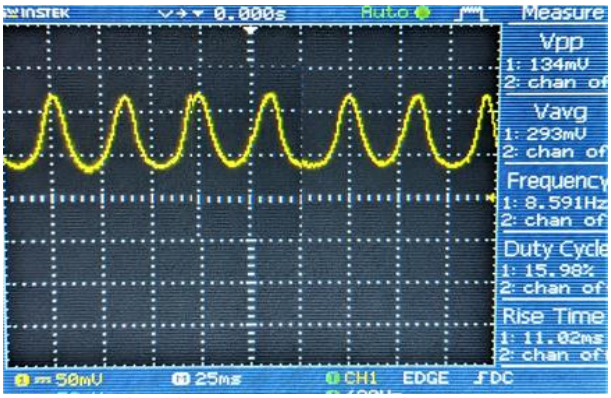

Fig. 9 Waveform for stainless steel beam of beam length 300mm

These results confirm the inverse relationship to beam length and vibration frequency, demonstrating that longer beams exhibit lower natural frequencies due to reduced stiffness and increased mass distribution. The consistency of waveform patterns validates the reliability of the proposed photodiode-based vibration sensing method for frequency extraction.

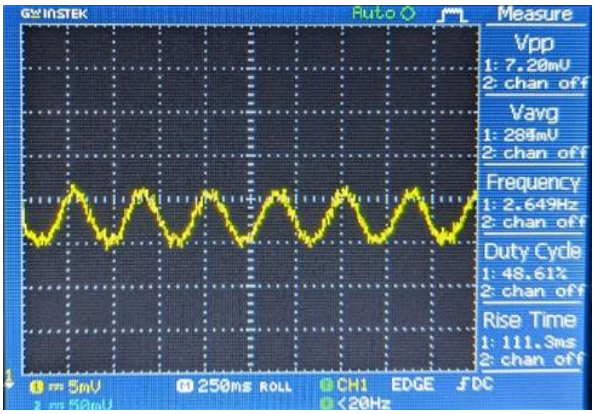

Fig. 10 Waveform for aluminium beam of beam length 500mm

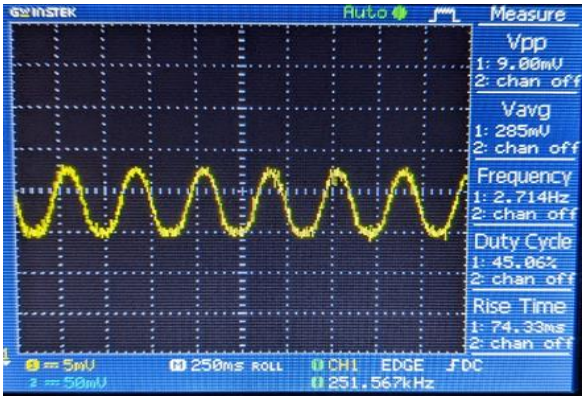

Fig. 11 Waveform for galvanized iron beam of beam length 500mm

4. Sentiment Cross-Fusion Network (SCFN)

The sentiment cross-fusion network is a Deep Learning Framework designed to learn time-dependent vibration patterns from photodiode voltage signals. It combines multi-scale temporal features and cross-path attention to enhance fault detection accuracy. SCFN effectively distinguishes subtle variations in vibration data caused by structural anomalies. This enables reliable, real-time predictive maintenance of cantilever beams.

$$X = \{x_1, x_2, \dots \dots x_T\}, \quad x_1 \epsilon R^d \tag{5}$$

Where X represents a sequence of vibration input signals from the Photodiode, x_t represents the input signal (voltage), T denotes the total number of time steps, and d represents the dimensionality of each input vector.

$$h_1 = ReLU(W_e\, x_t + b_e) \tag{6}$$

Where, h_t represents the encoded feature vector at time step t, W_e represents the weight matrix of the encoder layer $R^{d'Xd}$, b_e represents the bias vector, ReLU represents the rectified linear unit, and d' represents the dimension.

$$Attention(Q,K,V) = softmax[\left(\frac{QK^T}{\sqrt{d_k}}\right)V \tag{7}$$

Where, $Q=HW_Q$, $K=HW_K$, $V=HW_V$ represents the query, key, and value matrices, H represents matrix of hidden states $[h_1,h_2\dots..h_T]^T$, W_Q, W_K, W_V represents the learnable projection matrices, d_k represents the dimension of keys, softmax represents the activation function to normalise attention weights, attention () represents the output of attention layer capturing temporal dependencies.

$$Z = \lambda_1 . Attention_1 + \lambda_2 . Attention_2 \tag{8}$$

Where Z represents the final fused representation combining multiple attention heads, $Attention_1$ and $Attention_2$ represent the attention outputs from different pathways, and λ_1 and λ_2 represent the fusion weights.

$$\hat{y} = \begin{cases} softmax(W_0\, Z + b_0) & for\ classification \\ W_0\, Z + b_0 & for\ regression \end{cases} \tag{9}$$

Where, $\hat{y}$ Represents the output prediction, W_o represents the output weight matrix, and b_o represents the output bias term.

5. Optimization using the Improvised Arctic Fox Algorithm (IAFA)

The improvised arctic fox algorithm is a novel metaheuristic designed to optimize the performance of Deep Learning Models like SCFN by minimizing prediction error. It integrates chaotic mapping for exploration, Householder mirror reflection for efficient learning, and a Tangent Flight Search strategy to escape local optima. IAFA adaptively updates model parameters to enhance convergence and predictive accuracy in vibration pattern recognition. This makes it well-suited for real-time structural health monitoring applications.

$$\min_{\theta} L(y, \hat{y}\,(\theta)) \tag{10}$$

Where θ represents the model parameters of SCFN, y represents the ground truth vibration frequency/class, $\hat{y}(\theta)$ represents predicted output from SCFN, L represents the loss function.

$$Fitness = \frac{1}{N}\sum_{i=1}^{N} (y_i - \hat{y}_i)^2 \tag{11}$$

Where N indicates the number, y_i indicates true output, $\hat{y}_i$ Indicates predicted output.

$$Fitness = \frac{1}{N}\sum_{i=1}^{N}\sum_{j=1}^{C} y_{ij}\ \log(\widehat{y_{ij}}) \tag{12}$$

Where C indicates the number of classes, y_{ij} indicates the binary indicator, $\widehat{y_{ij}}$ Denotes predicted probability of the class j for sample i.

$$X_i^{t+1} = X_i^t + \alpha.\, C_t.\, (X_{best}^t - X_i^t) + \beta.\, H(X_i^t) + \gamma.\, TFS(X_i^t) \tag{13}$$

Where X_i^t represents the solution of the i^{th} fox at iteration t, X^t_{best} represents the best solution found so far, C_t represents the chaotic coefficient, α, β,γ represent the control parameters for balance and exploitation, $H(X^t_i)$ represents the householder mirror reflection learning component, and $TFS(X^t_i)$ represents the Tangent Flight Search operator for exploration.

$$L_{MSE} = \frac{1}{T}\sum_{i=1}^{T} (y_i - \hat{y}_i)^2 \tag{14}$$

Where LMSE represents the mean squared error loss, T indicates the total number, yt indicates the true (actual) vibration value, and y^t indicates the predicted vibration value by SCFN.

$$L_{CrossEntropy} = -\sum_{i=1}^{T} y_i \log(\hat{y}_i \tag{15}$$

Where $L_{crossEntropy}$ represents the cross-entropy loss.

$$\Theta^{*} = \underset{\theta}{\operatorname{argmin}}\, L(\theta) \quad (16)$$

Where θ represents the set of SCFN hyperparameters, L(θ)represents the total loss of the SCFN model using hyperparameters θ,θ* represents the optimal hyperparameter set that minimizes the loss, and argmin represents the operator that returns the value of θ for which the loss is minimum.

Table 4. Pseudocode for the improvised arctic fox algorithm

Input

Objective function L(θ) based on SCFN loss
Search Space S(parameter change for SCFN)
Max Iterations T
Population size N
Initial Chaotic value Co Є(0,1)

Output
Optimized SCFN weights θ*

Steps

1. Initialize fox population, P={ $\theta_1, \theta_2, \ldots\ldots \theta\_N$} randomly in S
2. Evaluate fitness in each using $L(\theta_i)$=MSE or cross entropy loss from SCFN
3. θ*= argmin{ $L(\theta_i)$: θ_i Є P
4. for t= 1 to T do
5. Update chaotic coefficient C_i+1= μ * C_t * (1- C_t) //logistic map
6. For each θ_i Є P do
7. Determine search mode: Mode(t)← Δ Mode(θi,t, C_t)
8. Switch Mode(t)
9. Case Exploration
10. θi_new= θi - ή ∇ L(θi) + α* sin(ω*t+ψ)+β*Z_t // Z_t is random vector
11. case exploitation
12. Sample Levy flight step:s_t Ŀ(c,μ)
13. θi_new= θi + s_t* θ* //step towards best
14. case Evasion
15. Generate random noise, dw_1 – N(0,1)
16. θi_new= θi+ √2D * dW_t
17. Apply Householder learning
18. H(θi)- θi -2*(vT θi)* v where v is householder vector
19. Combine:
20. θi_new← θi_new+ H(θi)+ TFS(θi)
21. θi←θi_new
22. If L(θi)< L(θ*) then
23. θ*← θi
24. end if
25. end if
26. end for
27. end for
28. Return optimized SCFN weights θ*

Table 4 illustrates the pseudocode of the IAFA designed to optimize the SCFN by minimizing its loss function. Initially, a population of SCFN weights is randomly generated within the search space, and the fitness is evaluated using the SCFN loss. The best solution is selected, and a logistic chaotic map updates a dynamic coefficient C_t to enhance global search behavior. Based on C_t and iteration count, the algorithm switches between three search modes: Exploration (gradient-based update with sinusoidal motion and random noise), Exploitation (stepwise update using Lévy flight toward the best solution), and Evasion (random walk using Gaussian noise). To further enrich the search space, Householder reflection and Tangent Flight Search are integrated, producing transformed updates. These transformations are accepted only if they lie within bounds and offer improved fitness. The process iterates until convergence, returning the optimized SCFN weight vector θ* for high-accuracy vibration pattern classification.

6. Results and Analysis

The results confirm that the photodiode-based method accurately detects the natural frequencies of cantilever beams, closely matching analytical, simulation, and accelerometer data. The SCFN model, when optimized using the IAFA, achieves improved prediction accuracy and faster convergence. This integrated approach proves effective for scalable, real-time, and non-contact vibration monitoring. However, limitations like photodiode active area and sensitivity to alignment must be considered for broader applications.

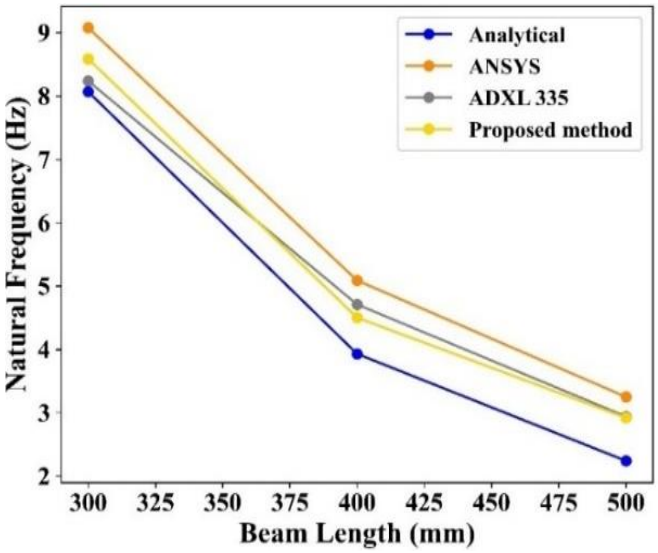

Fig. 12 Comparison of different approaches for SS304 beam for various beam lengths

Figure 12 compares natural frequencies of SS304 cantilever beams at lengths of 300 mm, 400 mm, and 500 mm using four different methods. At 300 mm, the analytical method gives 8.07 Hz, ANSYS simulation shows 9.08 Hz, ADXL335 measures 8.24 Hz, and the proposed photodiode-based method gives 8.59 Hz. At 400 mm, the corresponding frequencies are 3.93 Hz (analytical), 5.09 Hz (ANSYS), 4.71 Hz (ADXL335), and 4.502 Hz (proposed). For 500 mm, the methods yield 2.24 Hz, 3.25 Hz, 2.94 Hz, and 2.92 Hz, respectively. The proposed method shows close agreement with ADXL335 and ANSYS, validating its accuracy as presented in Table 5.

Table 5. Natural frequency of the cantilever beam made of SS304 obtained by different methods

Length of beam from fixed end, mm	Natural frequency in Hz			
	Analytical method	ANSYS	ADXL 335	Proposed method
300	8.07	9.08	8.24	8.59
400	3.93	5.09	4.71	4.502
500	2.24	3.25	2.94	2.92

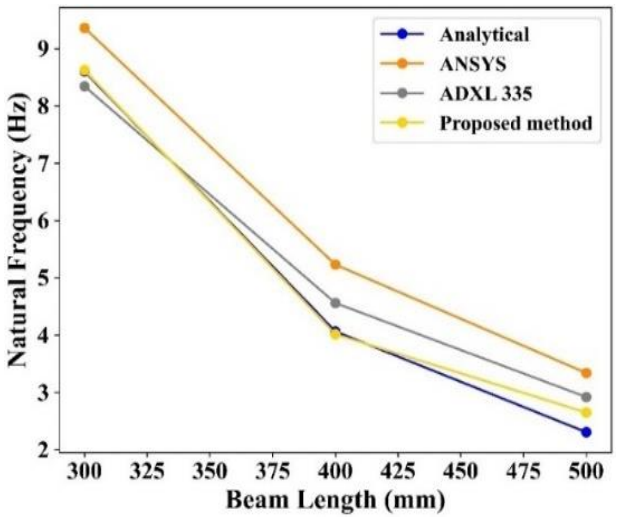

Fig. 13 Comparison of different approaches for the aluminum beam for various beam lengths

Figure 13 shows that the aluminium cantilever beams, the natural frequency at 300 mm is found to be 8.60 Hz (analytical), 9.36 Hz (ANSYS), 8.34 Hz (ADXL335), and 8.621 Hz (proposed method). At 400 mm, the frequencies are 4.065 Hz, 5.23 Hz, 4.56 Hz, and 4.016 Hz, respectively. For a 500 mm length, the values recorded are 2.307 Hz (analytical), 3.34 Hz (ANSYS), 2.92 Hz (ADXL335), and 2.649 Hz (proposed method). The proposed photodiode-based technique closely aligns with other established methods, confirming its reliability, as presented in Table 6.

Table 6. Natural frequency of the cantilever beam made of aluminium obtained by different methods

Length of beam from fixed end, mm	Natural frequency in Hz			
	Analytical method	ANSYS	ADXL 335	Proposed method
300	8.60	9.36	8.34	8.621
400	4.065	5.23	4.56	4.016
500	2.307	3.34	2.92	2.649

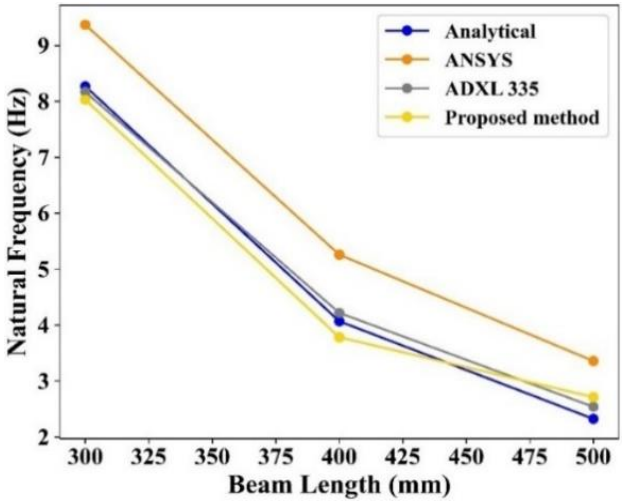

Fig. 14 Comparison of different approaches for GI beam for various beam lengths

Figure 14 shows the GI Cantilever Beams, the natural frequency at 300 mm is observed as 8.27 Hz (analytical), 9.37 Hz (ANSYS), 8.17 Hz (ADXL335), and 8.031 Hz (proposed method). At 400 mm length, the respective values are 4.07 Hz, 5.26 Hz, 4.22 Hz, and 3.784 Hz. For 500 mm, the frequencies recorded are 2.325 Hz (analytical), 3.36 Hz (ANSYS), 2.54 Hz (ADXL335), and 2.714 Hz (proposed). The proposed optical method shows close agreement with standard approaches, validating its accuracy for GI beam vibration analysis presented in Table 7.

Table 7. Natural frequency of the cantilever beam made of Galvanized Iron obtained by different methods

Length of beam from fixed end, mm	Natural frequency in Hz			
	Analytical method	ANSYS	ADXL 335	Proposed method
300	8.27	9.37	8.17	8.031
400	4.07	5.26	4.22	3.784
500	2.325	3.36	2.54	2.714

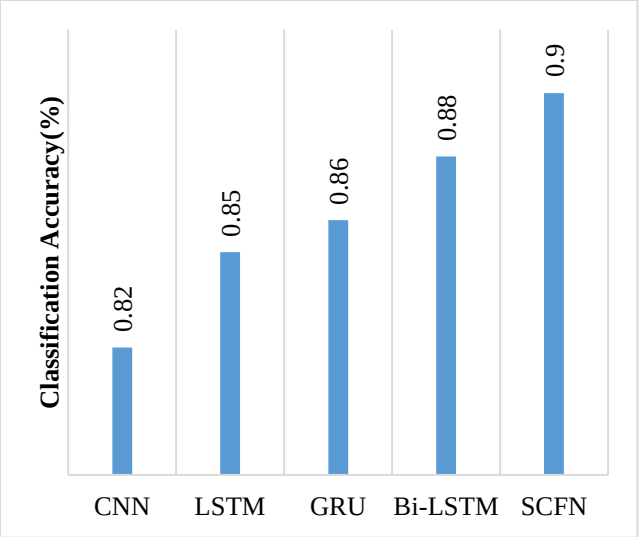

Fig. 15 Classification accuracy comparison of different deep learning models for vibration signal analysis

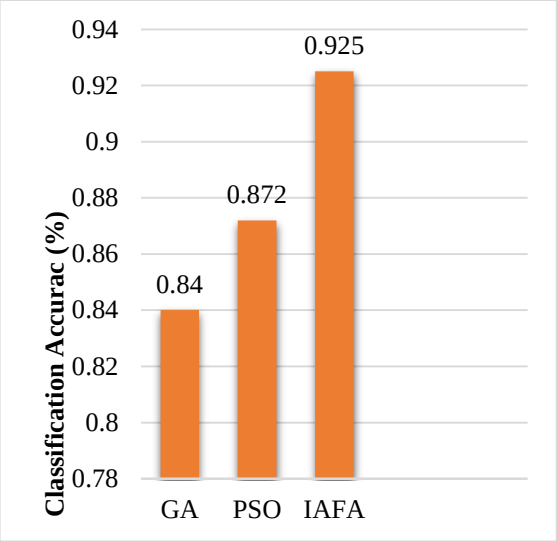

Fig. 16 Accuracy comparison of optimization using GA, PSO, AND IAFA

Figure 15 illustrates the classification accuracy of various Deep Learning Models applied to vibration data. The CNN model achieves an accuracy of 0.82%, LSTM improves this to 0.85%, and GRU further increases it to 0.86%.

The Bi-LSTM model performs even better with 0.88%, while the proposed SCFN attains the highest accuracy of 0.90%, demonstrating its superior ability to capture structural vibration patterns.

Figure 16 illustrates the comparative accuracy of three optimization techniques. The Genetic Algorithm (GA) achieved an accuracy of approximately 0.840%, Particle Swarm Optimization (PSO) improved to around 0.872%, while the proposed IAFA attained the highest accuracy of about 0.925%. This demonstrates IAFA's superior performance in enhancing prediction precision for vibration analysis.

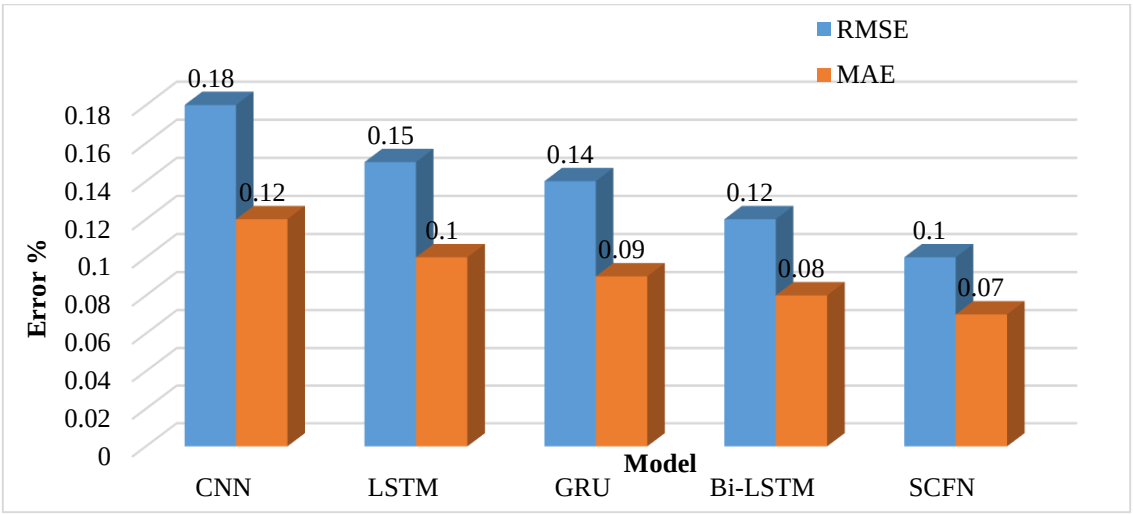

Fig. 17 RMSE and MAE error comparison of deep learning models for vibration prediction

Figure 17 compares the Root Mean Square Error (RMSE) and MAE of different deep learning models. CNN shows the highest errors with RMSE of 0.18 and MAE of 0.12, followed by LSTM (0.15, 0.10) and GRU (0.14, 0.09). Bi-LSTM achieves lower errors (0.12 RMSE, 0.08 MAE), while the proposed SCFN model records the lowest values of RMSE of 0.10 and Mean Absolute Error (MAE) of 0.07, highlighting its superior prediction accuracy.

Figure 18 illustrates the natural frequency variations for SS304, Aluminium, and Galvanized Iron Cantilever Beams of lengths 300 mm, 400 mm, and 500 mm. For SS304 at 300 mm, the experimental frequency is 8.8 Hz and predicted is 8.5 Hz; at 400 mm, 4.5 Hz and 4.2 Hz; at 500 mm, 2.7 Hz. Similar close agreement is observed for Aluminium (e.g., 8.3 Hz at 300 mm) and Galvanized Iron (8.0 Hz at 300 mm), confirming the accuracy of the photodiode-based predictive model.

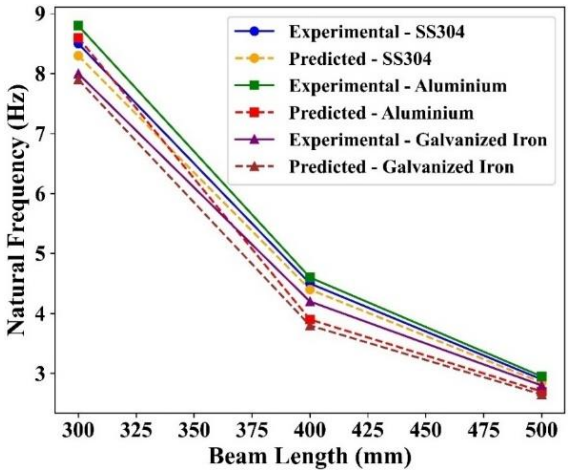

Fig. 18 Comparison of experimental and predicted natural frequencies for SS304, Aluminium, and galvanized iron beams

7. Conclusion

This research successfully demonstrated a novel, non-contact vibration sensing methodology that exploits the inherent non-uniform spectral responsivity of photodiodes for structural monitoring of cantilever beams. Unlike conventional systems that depend on physical contact or assume uniform photodiode sensitivity, the proposed method transforms spatial non-uniformity into a sensing advantage, enabling accurate detection of natural frequencies through optical voltage variations. The advantage of the proposed method over the existing optical-based approaches is that it reduces the number of optical components required for the vibration measurement and ensures the accuracy of the Measurement. Since the Photodiode serves both as the sensor and detector in this approach, there is no need for other vibration sensors like interferometers, fibre Bragg gratings, which form an integral part of optical-based vibration measurements in addition to a photodetector. Experimental investigations on SS304, Aluminium, and Galvanized Iron Beams of varying lengths showed that the proposed photodiode-based system provides natural frequency measurements within a 5% deviation from analytical, ANSYS, and ADXL335 accelerometer data, confirming its reliability and precision.

To augment fault detection and enable predictive maintenance, the voltage signals are processed using a Deep Learning model, SCFN, optimized by the IAFA. The SCFN achieved a classification accuracy of 0.90%, outperforming conventional models like CNN (0.82%), LSTM (0.85%), and Bi-LSTM (0.88%), while IAFA delivered the highest prediction accuracy of 92.1% with the lowest error metrics (RMSE = 0.10, MAE = 0.07). Overall, this integrated Photodiode–Deep Learning framework presents a scalable, intelligent, and real-time solution for structural health monitoring of Cantilever systems. However, practical challenges such as photodiode alignment precision and limited active area must be addressed to facilitate broader adoption in large-scale industrial or civil infrastructures. Future research may focus on extending this approach to multi-degree-of-freedom structures and incorporating advanced optical components for higher spatial resolution.

References

[1] Masoud Kharazan et al., "Nonlinear Vibration Analysis of a Cantilever Beam with Multiple Breathing Edge Cracks," *International Journal of Non-Linear Mechanics*, vol. 136, 2021. [CrossRef] [Google Scholar] [Publisher Link]

[2] V. Ondra, and B. Titurus, "Free Vibration and Stability Analysis of a Cantilever Beam Axially Loaded by an Intermittently Attached Tendon," *Mechanical Systems and Signal Processing*, vol. 158, pp. 1-21, 2021. [CrossRef] [Google Scholar] [Publisher Link]

[3] Muhammad Abuzar Khan et al., "Vibration Analysis of Damaged and Undamaged Steel Structure Systems: Cantilever Column and Frame" *Earthquake Engineering and Engineering Vibration*, vol. 19, pp. 725-737, 2020. [CrossRef] [Google Scholar] [Publisher Link]

[4] Mohammadali Ghafarian, Bijan Shirinzadeh, and Weichen Wei, "Vibration Analysis of a Rotating Cantilever Double-Tapered AFGM Nanobeam," *Microsystem Technologies*, vol. 26, pp. 3657-3676, 2020. [CrossRef] [Google Scholar] [Publisher Link]

[5] Ahmed E. Eldeeb, Dayu Zhang, and Ahmed A. Shabana, "Cross-Section Deformation, Geometric Stiffening, and Locking in the Nonlinear Vibration Analysis of Beams," *Nonlinear Dynamics*, vol. 108, pp. 1425-1445, 2022. [CrossRef] [Google Scholar] [Publisher Link]

[6] Marco Amabili et al., "Nonlinear Vibrations and Viscoelasticity of a Self-Healing Composite Cantilever Beam: Theory and Experiments," *Composite Structures*, vol. 294, 2022. [CrossRef] [Google Scholar] [Publisher Link]

[7] D. Gritsenko, J. Xu, and R. Paoli, "Transverse Vibrations of Cantilever Beams: Analytical Solutions with General Steady-State Forcing," *Applications in Engineering Science*, vol. 3, pp. 1-10, 2020. [CrossRef] [Google Scholar] [Publisher Link]

[8] Woojeong Sim et al., "Vibro-Impact Analysis of Two Adjacent Cantilever Beams," *Nonlinear Dynamics*, vol. 108, pp. 987-1004, 2022. [CrossRef] [Google Scholar] [Publisher Link]

[9] Ersin Aydin et al., "Optimization of Elastic Spring Supports for Cantilever Beams," *Structural and Multidisciplinary Optimization*, vol. 62, pp. 55-81, 2020. [CrossRef] [Google Scholar] [Publisher Link]

[10] Kok-Sing Lim et al., "Vibration Mode Analysis for a Suspension Bridge by Using Low-Frequency Cantilever-based FBG Accelerometer Array," *IEEE Transactions on Instrumentation and Measurement*, vol. 70, pp. 1-8, 2020. [CrossRef] [Google Scholar] [Publisher Link]

[11] Khaled Mohamed, Hassan Elgamal, and Sallam A. Kouritem, "An Experimental Validation of a New Shape Optimization Technique for Piezoelectric Harvesting Cantilever Beams," *Alexandria Engineering Journal*, vol. 60, no. 1, pp. 1751-1766, 2021. [CrossRef] [Google Scholar] [Publisher Link]

[12] JuatoWang et al., "A Novel Piezoelectric Energy Harvester with Different Circular arc Spiral Cantilever Beam," *IEEE Sensors Journal*, vol. 22, no. 11, pp. 11016-11022, 2022. [CrossRef] [Google Scholar] [Publisher Link]

[13] Zhen'an Jia et al., "A Two-Dimensional Cantilever Beam Vibration Sensor based on Fiber Bragg Grating," *Optical Fiber Technology*, vol. 61, 2021. [CrossRef] [Google Scholar] [Publisher Link]

[14] Xiaohao Li, Deyu Shi, and Zihang Yu, "Nondestructive Damage Testing of Beam Structure Based on Vibration Response Signal Analysis," *Materials*, vol. 13, no. 15, pp.1-13, 2020. [CrossRef] [Google Scholar] [Publisher Link]

[15] Duong Huong Nguyen et al., "Damage Evaluation of Free-Free Beam Based on Vibration Testing," *Applied Mechanics*, vol. 1, no. 2, pp. 142-152, 2020. [CrossRef] [Google Scholar] [Publisher Link]

[16] Siva Sankara Babu Chinka, Srinivasa Rao Putti, and Bala Krishna Adavi, "Modal Testing and Evaluation of Cracks on Cantilever Beam Using Mode Shape Curvatures and Natural Frequencies," *Structures*, vol. 32, pp. 1386-1397, 2021. [CrossRef] [Google Scholar] [Publisher Link]

[17] DevDatt Pathak et al., "Vibration Analysis of Cracked Cantilever Beam Using Response Surface Methodology," *Journal of Vibration Engineering & Technologies*, vol. 11, pp. 2429-2452, 2023. [CrossRef] [Google Scholar] [Publisher Link]

[18] Abdelwahhab Khatir et al., "A New Hybrid PSO-YUKI for Double Cracks Identification in CFRP Cantilever Beam," *Composite Structures*, vol. 311, pp. 1-28, 2023. [CrossRef] [Google Scholar] [Publisher Link]

[19] Hai Feng, Peng Liu, and Fujiang Cui, "A Novel Method for Damage Identification in Cantilever Beams using Generalized Energy Index and Deep Learning Model," *Measurement*, vol. 253, 2025. [CrossRef] [Google Scholar] [Publisher Link]

[20] Afandi Nur Aziz Thohari et al., "Crack Detection in Building through Deep Learning Feature Extraction and Machine Learning Approach," *Journal of Applied Informatics and Computing*, vol. 8, no. 1, pp. 1-6, 2024. [CrossRef] [Google Scholar] [Publisher Link]

[21] Siva Charan Kadagala et al., "Detection and Classification of Types of Cracks Using Deep Learning," *2024 IEEE International Conference on Information Technology, Electronics and Intelligent Communication Systems (ICITEICS)*, Bangalore, India, pp. 1-6, 2024. [CrossRef] [Google Scholar] [Publisher Link]

[22] Vishnu Harikumar, and C.R. Bijudas, "Digital Twin for Health Monitoring of a Cantilever Beam Using Support Vector Machine," *Journal of Vibration Engineering & Technologies*, vol. 13, 2025. [CrossRef] [Google Scholar] [Publisher Link]

[23] Xinyu Zhang, Hao Zhu, and Wei Xu, "Dynamic Response Prediction of a Cantilever Beam Under Different Boundary Constraints and Excitation Conditions Based on an Improved Physics-Informed Neural Network," *The Structural Design of Tall and Special Buildings*, vol. 34, no. 2, 2025. [CrossRef] [Google Scholar] [Publisher Link]

[24] Rakesh Katam, Venkata Dilip Kumar Pasupuleti, and Prafulla Kalapatapu, "SVM-Assisted Damage Identification in Cantilever Steel Beam using Vibration-Based Method," *Innovative Infrastructure Solutions*, vol. 9, 2024. [CrossRef] [Google Scholar] [Publisher Link]

[25] N.V.S. Shankar et al., "IoT for Vibration Measurement in Engineering Research," *Materials Today: Proceedings*, vol. 59, pp. 1792-1796, 2022. [CrossRef] [Google Scholar] [Publisher Link]